

Synthesis and Characterization of Trimetallic Rare Earth Orthoferrites, $\text{La}_x\text{Sm}_{1-x}\text{FeO}_3$

Enrico Traversa,^a Gualtiero Gusmano,^a Brigida Allieri,^b Laura E. Depero,^b
Luigi Sangaletti,^c Hiromichi Aono^d and Yoshihiko Sadaoka^d

^aConsorzio Interuniversitario Nazionale per la Scienza Tecnologia dei
Materiali (INSTM) & Dipartimento di Scienze e Tecnologie Chimiche,
Universita' di Roma "Tor Vergata," 00133 Roma, Italy

^bIstituto Nazionale per la Fisica della Materia (INFM) & Dipartimento di Ingegneria Meccanica,
Universita' di Brescia, 25123 Brescia, Italy

^cIstituto Nazionale per la Fisica della Materia (INFM) & Dipartimento di Matematica e Fisica,
Universita' Cattolica del Sacro Cuore, Via Trieste 17, 25121 Brescia, Italy

^dDepartment of Materials Science and Engineering, Faculty of Engineering,
Ehime University, Matsuyama 790-8577, Japan

(Received September 23, 1998)

Nanosized powders of trimetallic orthoferrites containing La and Sm in different ratios were synthesised by the thermal decomposition at low temperatures of the corresponding hexacyanocomplexes. The precursors and their decomposition products were analyzed by simultaneous thermogravimetric and differential thermal analysis (TG/DTA), x-ray diffraction (XRD) and Raman spectroscopy. Single phase trimetallic precursors and oxides were obtained. The crystal structure of the perovskitic oxides was orthorhombic, and the lattice parameters were affected by the ionic size of the rare earth elements present in the oxides. Raman spectroscopy showed a disorder effect in the vibrational bands with increasing the La content.

Key words : Perovskite, $\text{La}_x\text{Sm}_{1-x}\text{FeO}_3$, Raman spectroscopy, X-ray diffraction, Thermal decomposition

I. Introduction

Rare earth orthoferrites, LnFeO_3 , with perovskite-type structures are interesting materials for electroceramic applications due to their mixed conductivity.^{1,2)} These materials are known to display ionic and electronic defects,³⁾ which make these compounds important candidates for the development of many innovative technologies.⁴⁻¹⁰⁾

Heterometallic oxides, like rare earth orthoferrites, are conventionally prepared by the solid-state reaction at high temperatures of the corresponding single oxides. Problems such as a crystal growth, change of the atomic stoichiometric ratio, and ease for second phase formation are easily encountered.¹¹⁾ Chemical processing is being used to control the homogeneity and reproducibility of the ceramic products and to lower the synthesis temperature.¹²⁾ Several chemical methods have been proposed for the preparation of rare earth orthoferrites.¹³⁻¹⁶⁾

The preparation of LnFeO_3 and LnCoO_3 perovskite-type oxides by the thermal decomposition at low temperatures of the appropriate hexacyanocomplexes, readily precipitated from aqueous solution, was firstly proposed by Gallagher in 1968.¹⁷⁾ Recently, some of the authors of this paper have confirmed that rare earth perovskite-type oxides with relatively high specific surface area can be obtained using this preparation method.¹⁸⁻²⁰⁾ This method is very useful to

obtain homogeneous, nanosized rare earth orthoferrite powders at temperatures as low as 600°C.²¹⁻²³⁾ Moreover, this method allows the preparation of single-phase, trimetallic complexes, the decomposition of which may lead to the formation of single-phase, trimetallic perovskite-type oxides, containing either two rare earths and Co,²⁴⁻²⁶⁾ or one Ln and two transition metals (Fe and Co).²⁷⁻²⁹⁾ This is very interesting because the possibility to prepare trimetallic oxides gives the chance to modulate in a wide range the functional properties of the perovskitic oxides.

In this paper, we report the synthesis and the structural characterization by x-ray diffraction and Raman spectroscopy of trimetallic orthoferrites in the series $\text{La}_x\text{Sm}_{1-x}\text{FeO}_3$ ($x=0-1$), prepared by the thermal decomposition of the corresponding hexacyanocomplexes, $\text{La}_x\text{Sm}_{1-x}[\text{Fe}(\text{CN})_6] \cdot n\text{H}_2\text{O}$. We compare the results obtained with the data previously reported for the similar series containing Co instead of Fe.^{25,26)}

II. Experimental Procedure

The heteronuclear complexes, $\text{La}_x\text{Sm}_{1-x}[\text{Fe}(\text{CN})_6] \cdot n\text{H}_2\text{O}$ ($x=0, 0.2, 0.4, 0.5, 0.6, 0.8, \text{ and } 1$), were synthesized at room temperature by mixing aqueous solutions of appropriate amounts of $\text{La}(\text{NO}_3)_3 \cdot 6\text{H}_2\text{O}$, $\text{Sm}(\text{NO}_3)_3 \cdot 6\text{H}_2\text{O}$, and $\text{K}_3\text{Fe}(\text{CN})_6$. After the mixture was stirred at room temperature for 30 minutes, the precipitate obtained was collected by

suction filtration and then washed with water, ethanol and diethyl ether, before drying in air at 50°C. Atomic absorption analysis showed that the potassium content of the purified complexes was lower than 0.05 wt%. The complexes were decomposed at a rate of 5°C/min in air up to selected temperatures in the range from 700°C to 1000°C, at intervals of 100°C, held for 60 min., in order to obtain the trimetallic orthoferrites in the series $\text{La}_x\text{Sm}_{1-x}\text{FeO}_3$.

The thermal decomposition behaviour of the complexes was studied by simultaneous thermogravimetric and differential thermal analysis (TG/DTA), performed in flowing air with a heating rate of 5°C/min. The characterization of the structure of the complexes and of their decomposition products was carried out by x-ray diffraction (XRD), using $\text{Cu K}\alpha$ ($\lambda=0.154$ nm) radiation. Microraman spectra were collected with a DILOR Labram spectrometer confocally coupled with an optical microscope. The $\lambda=632.8$ nm line of a 10 mW He-Ne laser was used as excitation source. Rejection of the elastic peak was achieved by using a holographic notch filter, which resulted in a cutting of the scattered signal below 100 cm^{-1} . The laser power on the sample was kept below 0.5 mW mm^{-2} .

III. Results and Discussion

Fig. 1 shows the XRD results for the $\text{La}_x\text{Sm}_{1-x}[\text{Fe}(\text{CN})_6] \cdot n\text{H}_2\text{O}$ complexes. The XRD patterns for the complexes having x from 0 to 0.6 showed that they crystallized in the orthorhombic symmetry. For LnFe-complexes with Ln=La, Ce, Pr, and Nd, Hulliger *et al.*³⁰ determined two types of crystal structures on single crystals, depending on the number of crystallization water molecules, *i.e.*, hexagonal for $n=5$ and orthorhombic for $n=4$. The number of crystalli-

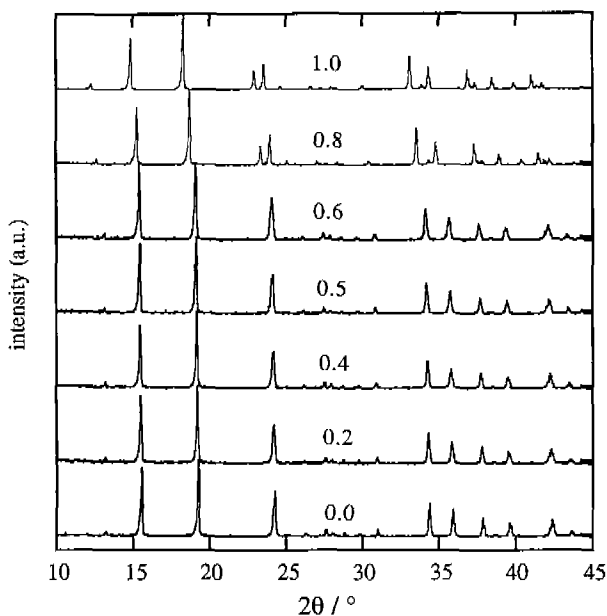


Fig. 1. XRD profiles of the $\text{La}_x\text{Sm}_{1-x}[\text{Fe}(\text{CN})_6] \cdot n\text{H}_2\text{O}$ complexes (x values are indicated in the figure).

zation water molecules was estimated to be 4 from TGA measurements, in agreement with the results reported in the literature. On the other hand, the XRD patterns of the LaFe- and $\text{La}_{0.8}\text{Sm}_{0.2}\text{Fe}$ -complexes showed that they consisted of a mixture of hexagonal and orthorhombic structures, as discussed elsewhere.²⁹

A gradual shift of the XRD peaks towards higher values of 2θ with increasing the Sm content was observed, as shown in Fig. 1. The FWHM (full width at half maximum) of the major XRD peaks for orthorhombic structure was not significantly affected by the x value. We could thus assume that the $\text{La}_x\text{Sm}_{1-x}\text{Fe}$ -complexes were made of a single crystalline phase. Hulliger *et al.* demonstrated that a linear relationship exists between the lattice parameters and the ionic radius of the rare earth element for the Ln ferri- and chromicyanides.³⁰ The same linear dependence of the lattice parameters was observed for trimetallic cobalt-cyanides, when plotted as a function of the effective radii of the rare earth ions, defined as $r_{\text{eff}}=x r_{\text{Ln}'}+(1-x)r_{\text{Ln}}$.²⁶ For the radii of the Ln ions, the values reported by Shannon and Prewitt were used.^{31,32} We tried to confirm this behaviour for the complexes in the $\text{La}_x\text{Sm}_{1-x}\text{Fe}$ series. The lattice parameters of the complexes were determined by assuming the orthorhombic crystalline structure and reported as a function of the effective radius parameter of the rare earth ions in the complexes, defined as $x r_{\text{La}}+(1-x)r_{\text{Sm}}$, as shown in Fig. 2. In Fig. 2, the linear fitting extrapolated for the complexes in the LnFe series³³ is also reported. All the prepared $\text{La}_x\text{Sm}_{1-x}\text{Fe}$ -complexes with orthorhombic structure fit well the linear relationship established for the LnFe-complexes. This confirms the results obtained for trimetallic complexes with Co.²⁶ The lattice parameters of the $\text{Ln}'\text{Ln}''_{1-x}\text{Fe}$ -complexes with orthorhombic structure are determined by the size of the rare-earth-metal ions present

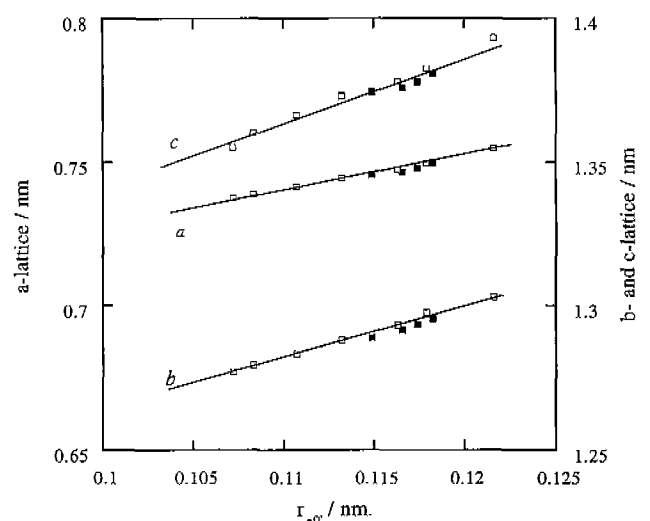


Fig. 2. Correlation between the lattice parameters and r_{eff} , defined as $x r_{\text{La}}+(1-x)r_{\text{Sm}}$, for the $\text{La}_x\text{Sm}_{1-x}\text{Fe}$ -complexes (closed symbols); the lattice parameters for the LnFe-complexes (open symbols) are also reported together with their linear fitting (from ref. 31).

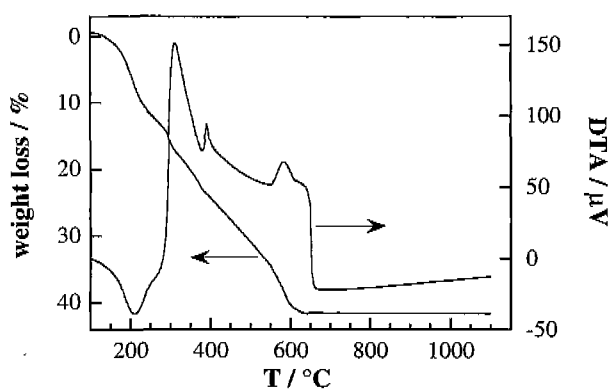


Fig. 3. DTA and TG curves of the $\text{La}_{0.6}\text{Sm}_{0.4}[\text{Fe}(\text{CN})_6]\cdot 4\text{H}_2\text{O}$ heteronuclear complex, measured in flowing air, at the heating rate of $5^\circ\text{C}/\text{min}$.

in the molecule.

Fig. 3 shows the TG and DTA curves for the $\text{La}_{0.6}\text{Sm}_{0.4}\text{Fe}$ -complex, as an example for the series of the complexes. The TG curve shows that the weight loss started slowly at about 110°C , followed by a faster loss which was completed at about 290°C , accompanied by an endothermic effect in the DTA curve with its maximum at about 210°C . This weight loss can be ascribed to the loss of crystallization water. The weight loss continued up to about 650°C , with three different slopes. Each change of slope was in correspondence of an exothermic peak in the DTA curve. The first exothermic peak, at about 310°C , can be associated with the decomposition of the cyanide groups.³³ In correspondence of the final weight loss the DTA curve showed a broad exothermic peak, with its maximum at about 580°C in the DTA curve. This weight loss can be ascribed to the

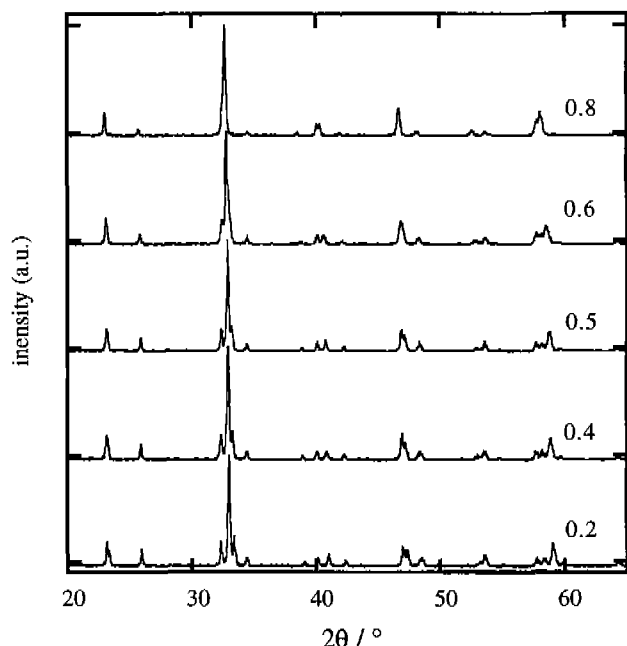


Fig. 4. XRD profiles of the $\text{La}_x\text{Sm}_{1-x}[\text{Fe}(\text{CN})_6]\cdot n\text{H}_2\text{O}$ complexes decomposed at 1000°C (x values are indicated in the figure).

loss of carbonate groups adsorbed on the oxide surface.³⁴ At temperatures above 650°C the weight loss remained constant. The total weight loss was 41.6%, in good agreement with the theoretical loss (42.12%) calculated for the formation of $\text{La}_{0.6}\text{Sm}_{0.4}\text{FeO}_3$ from the complex with 4 molecules of crystallization water. For the other complexes, the trend is that the weight loss increased with increasing the La content, in agreement with the theoretical values. On the other hand, the temperature at which the weight loss remained constant slightly increased with increasing the Sm content.

XRD results on the decomposition products of the complexes showed that single-phase trimetallic orthoferrites in orthorhombic symmetry were already formed above 650°C . With increasing the decomposition temperatures, crystallinity of the samples improved. Fig. 4 shows the XRD patterns of the $\text{La}_x\text{Sm}_{1-x}\text{Fe}$ -complexes decomposed at 1000°C . For $x=1$ and $x=0$ (data not reported in the figure), the XRD patterns were in agreement with the data reported in the literature for LaFeO_3 (JCPDS file No. 37-1493, orthorhombic), and SmFeO_3 (JCPDS file No. 39-1490, orthorhombic), respectively. The XRD spectra of the decomposed complexes prepared by partially replacing Sm with La were in between the patterns observed for LaFeO_3 and SmFeO_3 . The XRD peaks shifted to lower diffraction angles as the La content increased. One of the most interesting features observed in the rare earth perovskite-type family of compounds is the linear dependence of the lattice parameters on the effective radii of the rare earth ions, defined as $r_{\text{eff}} = x r_{\text{La}^{3+}} + (1-x)r_{\text{Sm}^{3+}}$, as observed for the trimetallic rare earth orthocobaltites.²⁶ From the XRD results reported above, a correlation between the Ln ionic radii and the crystal structure of the orthoferrites can be clearly suggested. Again, the lattice parameters of the orthorhombic structures were

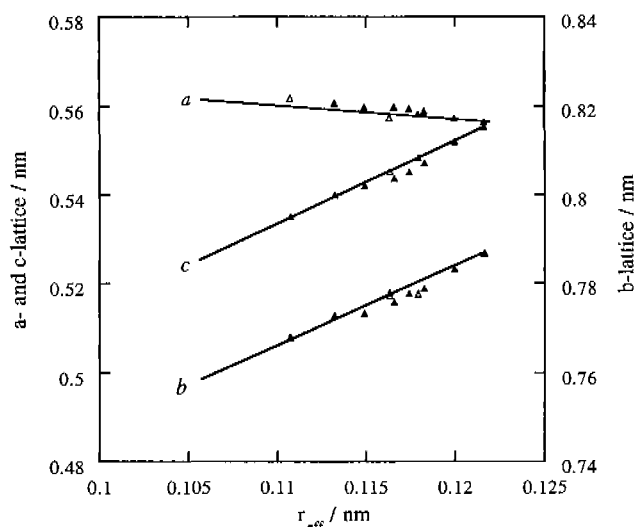


Fig. 5. Correlation between the lattice parameters and r_{eff} , defined as $xr_{\text{La}^{3+}} + (1-x)r_{\text{Sm}^{3+}}$, for the $\text{La}_x\text{Sm}_{1-x}\text{Fe}$ -complexes decomposed at 1000°C (closed symbols); the lattice parameters for LnFeO_3 series (open symbols) are also reported together with their linear fitting (from ref. 31).

determined and reported as a function of r_{eff} , defined as $x r_{\text{La}} + (1-x) r_{\text{Sm}}$, as shown in Fig. 5, where the lattice parameters of the LnFeO_3 oxides and their linear fitting³⁴⁾ are also reported. The trend for the variation with r_{eff} of the lattice parameters of the $\text{La}_x\text{Sm}_{1-x}\text{FeO}_3$ oxides is exactly the same as for LnFeO_3 oxides. The observed correlation suggests that the lattice parameters of the $\text{La}_x\text{Sm}_{1-x}\text{FeO}_3$ orthoferrites are primarily influenced by the size of the rare-earth metal ions present in the molecule, more than by their chemical nature. The effective radius of the Ln ion is a powerful parameter for elucidating the role played by the rare-earth elements.

Fig. 6 shows the Raman spectroscopy data for the $\text{La}_x\text{Sm}_{1-x}\text{FeO}_3$ Fe-complexes decomposed at 900°C. Raman spectroscopy data on rare-earth orthoferrites are reported in the relevant literature for TbFeO_3 , DyFeO_3 , TmFeO_3 ,³⁵⁾ LuFeO_3 ,³⁶⁾ and ErFeO_3 .³⁷⁾ A thorough analysis of the Raman bands observed for the $\text{La}_x\text{Sm}_{1-x}\text{FeO}_3$ samples goes beyond the purpose of the present study. However some useful remarks can be made by observing the behavior of the Raman bands with decreasing the content of Sm. Sharp Raman bands were observed for the SmFeO_3 sample. The increase in the La content resulted in a broadening of the Raman bands. This effect can be ascribed to a disorder effect induced by the substitutio of Sm with La cation in the SmFeO_3 lattice.

Microraman mapping was also performed in order to check the sample homogeneity. Apart from the sample with $x=0.2$, which showed some inhomogeneity in the Raman spectra, the

other sample did not show significant changes in the spectral features of spectra collected at different points.

According to the linear relationship observed for the lattice parameters on the effective radius of the rare earth ions, we tried to follow the same approach by treating the Raman data, introducing the concept of the effective cation mass, defined as $m_{\text{eff}} = xm_{\text{La}} + (1-x)m_{\text{Sm}}$, for the discussion of the Raman bands behavior for the present samples.

The Raman modes above 200 cm^{-1} showed in general an increase in frequency with increasing the effective mass m_{eff} of the $\text{La}_{1-x}\text{Sm}_x$ "cation." This effect has been already observed for TbFeO_3 , DyFeO_3 , TmFeO_3 , and LuFeO_3 , and explained by observing that a systematic decrease in the cell size with the mass of the Ln^{3+} ions may cause a slight increase in the Ln-O and Fe-O force constants.^{35,36)}

Therefore, if one assumes that most of the features above 200 cm^{-1} are associated with the vibration of oxygen ions (because of their relatively high frequency these modes are most likely associated with the light oxygen atoms rather than with the rare earth), their frequency is expected to increase with increasing the mass of the Ln^{3+} ion, because of the increase in the Ln-O and Fe-O force constants. This interpretation is also in agreement with the observed broadening of the Raman modes above 200 cm^{-1} with increasing the La content. Indeed, the presence of La ions at Sm lattice sites may cause local distortions of the cation coordination octahedra and therefore a broadening of the Raman bands ascribed to the motion of oxygen ions.

A broad electronic continuum was occasionally observed below the phonon bands. This kind of feature was also systematically observed in the Raman scattering of the LnTiO_3 family of Mott-Hubbard insulators ($\text{Ln}=\text{La}, \text{Ce}, \text{Pr}, \text{Nd}, \text{Sm}, \text{Gd}$) and ascribed to free-electron scattering.³⁸⁾ Though this aspect deserves further investigations, the presence of a broad continuum observed in orthoferrites may indicate the presence of charge carriers induced by oxygen substoichiometry, for example.

IV. Conclusions

Trimetallic orthoferrites in the $\text{La}_x\text{Sm}_{1-x}\text{FeO}_3$ series were synthesised by the thermal decomposition at low temperatures (650°C) of the corresponding hexacyanocomplexes, $\text{La}_x\text{Sm}_{1-x}[\text{Fe}(\text{CN})_6] \cdot n\text{H}_2\text{O}$. The major role played by the ionic radii of the Ln^{3+} ions on the formation of the orthoferrites has been identified. The size of the ions present in the perovskitic oxides is more important than their chemical nature for the determination of the stable crystalline structure. Raman spectroscopy showed a disorder effect in the vibrational bands with increasing the La content. These materials possess promising characteristics for their applications as electroceramics.

Acknowledgements

The present work was partly supported by a Grant-in-

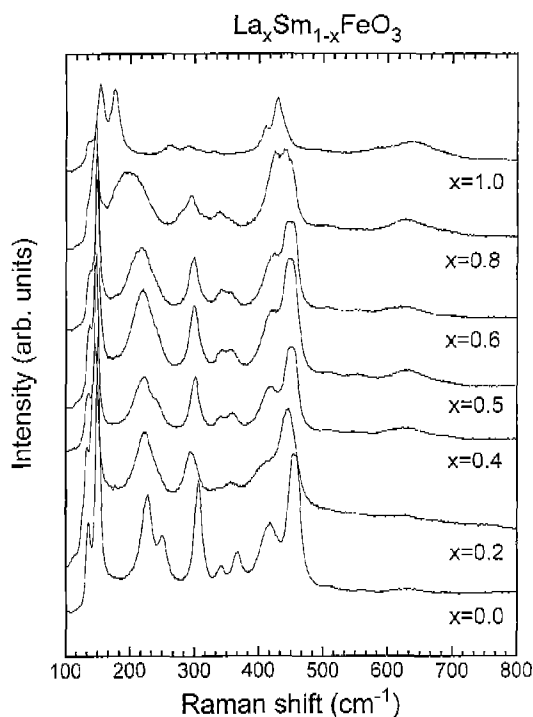


Fig. 6. Raman spectra of the $\text{La}_x\text{Sm}_{1-x}[\text{Fe}(\text{CN})_6] \cdot n\text{H}_2\text{O}$ complexes decomposed at 900°C (x values are indicated in the figure).

Aids for Scientific Research (Nos. 1065081 and 10045045) from the Ministry of Education, Science and Culture of Japan, and partly by the National Research Council of Italy (CNR), under the auspices of the Targeted Project "Special Materials for Advanced Technology II" (MSTA 2), and the Ministry of University and Research of Italy (MURST).

References

1. E. D. Wachsman, "Oxide-Ion Conducting Ceramics: Defect Chemistry and Applications," pp. 129-143 in *Progress in Ceramic Basic Science: Challenge Toward the 21st Century*. Ed. by T. Hirai, S.I. Hirano and Y. Takeda. The Ceramic Society of Japan, Tokyo, Japan, 1996.
2. J. W. Stevenson, T. R. Armstrong, R. D. Carneim, L. R. Pederson and W. J. Weber, "Electrochemical Properties of Mixed Conducting Perovskites $\text{La}_{1-x}\text{M}_x\text{Co}_{1-y}\text{Fe}_y\text{O}_{3-d}$ (M=Sr, Ba, Ca)," *J. Electrochem. Soc.*, **143**, 2722-2729 (1996).
3. M. Cherry, M. S. Islam and C. R. A. Catlow, "Oxygen Ion Migration in Perovskite-Type Oxides," *J. Solid State Chem.*, **118**, 125-132 (1995).
4. N. O. Minh, "Ceramic Fuel Cell," *J. Am. Ceram. Soc.*, **76**, 563-588 (1993), and references cited therein.
5. J. G. McCarty and H. Wise, "Perovskite Catalysts for Methane Combustion," *Catalysis Today*, **8**, 231-248 (1990).
6. C. B. Alcock, R. C. Doshi and Y. Shen, "Perovskite Electrodes for Sensors," *Solid State Ionics*, **51**, 281-289 (1992).
7. Y. Teraoka, T. Nobunaga and N. Yamazoe, "Effect of Cation Substitution on the Oxygen Semipermeability of Perovskite-Type Oxides," *Chem. Lett.*, 503-506 (1988).
8. U. Balachandran, J. T. Dusek, S. M. Sweeney, R. B. Poeppel, R. L. Mieville, P. S. Maiya, M. S. Kleefisch, S. Pei, T. P. Kobylinski, C. A. Udovch and A. C. Bose, "Methane to Syn-gas via Ceramic Membranes," *Am. Ceram. Soc. Bull.*, **74**(1), 71-75 (1995).
9. T. Arakawa, H. Kurachi and J. Shiokawa, "Physicochemical Properties of Rare Earth Perovskite Oxide Used as Gas Sensor Material," *J. Mater. Sci.*, **4**, 1207-1210 (1985).
10. C. Yu, Y. Shimizu and H. Arai, "Investigation on a Lean-Burn Oxygen Sensor Using Perovskite-Type Oxides," *Chem. Lett.*, 563-566 (1986).
11. M. Kakihana, "Sol-Gel Preparation of High Temperature Superconducting Oxides," *J. Sol-Gel Sci. Technol.*, **6**, 7-55 (1996).
12. B. I. Lee and E. J. Pope (eds.), *Chemical Processing of Ceramics*. Marcel Dekker, New York, 1994.
13. H. M. Zhang, Y. Teraoka and N. Yamazoe, "Preparation of Perovskite-Type Oxides with Large Surface Area by Citrate Process," *Chem. Lett.*, 665-668 (1987).
14. M. Inoue, T. Nishikawa, T. Nakamura and T. Inui, "Glycothermal Reaction of Rare-Earth Acetate and Iron Acetylacetonate: Formation of Hexagonal REFeO_3 ," *J. Am. Ceram. Soc.*, **80**, 2157-2160 (1997).
15. T. Tao, A. Ariyoshi and T. Inui, "Synthesis of LaMeO_3 (Me=Cr, Mn, Fe, Co) Perovskite Oxides from Aqueous Solutions," *J. Am. Ceram. Soc.*, **80**, 2441-1444 (1997).
16. C. Vázquez-Vázquez, P. Kögerler, M.A. López-Quintela, R. D. Sánchez and J. Rivas, "Preparation of LaFeO_3 Particles by Sol-Gel Technology," *J. Mater. Res.*, **13**, 451-456 (1998).
17. P. K. Gallagher, "A Simple Technique for the Preparation of R. E. FeO_3 and R. E. CoO_3 ," *Mater. Res. Bull.*, **3**, 225-232 (1968).
18. S. Nakayama, M. Sakamoto, K. Matsuki, Y. Okimura, R. Ohsumi, Y. Nakayama and Y. Sadaoka, "Preparation of Perovskite-Type LaFeO_3 by Thermal Decomposition of Heteronuclear Complex, $\{\text{La}[\text{Fe}(\text{CN})_6] \cdot 5\text{H}_2\text{O}\}_x$," *Chem. Lett.*, 2145-2148 (1992).
19. Y. Sadaoka, K. Watanabe, Y. Sakai and M. Sakamoto, "Thermal Decomposition Behavior of Heteronuclear Complexes, $\text{Ln}[\text{Co}(\text{CN})_6] \cdot n\text{H}_2\text{O}$ (Ln=La-Yb)," *J. Ceram. Soc. Jpn.*, **103**, 519-522 (1995).
20. Y. Sadaoka, K. Watanabe, Y. Sakai and M. Sakamoto, "Preparation of Perovskite-Type Oxides by Thermal Decomposition of Heteronuclear Complexes, $\{\text{Ln}[\text{Fe}(\text{CN})_6] \cdot n\text{H}_2\text{O}\}_x$," *J. Alloys and Compounds*, **224**, 194-198 (1995).
21. E. Traversa, M. Sakamoto and Y. Sadaoka, "Mechanism of LaFeO_3 Perovskite-Type Oxide from the Thermal Decomposition of d-f Heteronuclear Complex $\text{La}[\text{Fe}(\text{CN})_6] \cdot 5\text{H}_2\text{O}$," *J. Am. Ceram. Soc.*, **79**, 1401-1404 (1996).
22. E. Traversa, P. Nunziante, M. Sakamoto, Y. Sadaoka, M. C. Carotta and G. Martinelli, "Thermal Evolution of the Microstructure of Nanosized LaFeO_3 Powders from the Thermal Decomposition of a Heteronuclear Complex, $\text{La}[\text{Fe}(\text{CN})_6] \cdot 5\text{H}_2\text{O}$," *J. Mater. Res.*, **13**, 1335-1344 (1998).
23. M. C. Carotta, G. Martinelli, Y. Sadaoka, P. Nunziante and E. Traversa, "Gas-Sensitive Electrical Properties of Perovskite-Type SmFeO_3 Thick Films," *Sensors and Actuators B*, **48**, 270-276 (1998).
24. Y. Sadaoka, E. Traversa and M. Sakamoto, "Preparation and Characterization of Heteronuclear Hexacyano Complexes, $\text{Ln}_x\text{Sm}_{1-x}[\text{Co}(\text{CN})_6] \cdot n\text{H}_2\text{O}$ (Ln=La, Er and Yb)," *Chem. Lett.*, 177-78, 1996.
25. Y. Sadaoka, E. Traversa and M. Sakamoto, "Preparation and Structural Characterization of Perovskite-type $\text{La}_x\text{Ln}_{1-x}\text{CoO}_3$ by the Thermal Decomposition of Heteronuclear Complexes, $\text{La}_x\text{Ln}_{1-x}[\text{Co}(\text{CN})_6] \cdot n\text{H}_2\text{O}$ (Ln=Sm and Ho)," *J. Alloys and Compounds*, **240**, 51-59 (1996).
26. Y. Sadaoka, E. Traversa and M. Sakamoto, "Preparation and Characterization of Perovskite-type $\text{Ln}'\text{Ln}''_{1-x}\text{CoO}_3$ for Electroceramic Applications," *J. Mater. Chem.*, **6**, 1355-1360 (1996).
27. Y. Sadaoka, E. Traversa, P. Nunziante and M. Sakamoto, "Preparation of Perovskite-Type $\text{LaFe}_x\text{Co}_{1-x}\text{O}_3$ by Thermal Decomposition of Heteronuclear Complex, $\text{La}[\text{Fe}_x\text{Co}_{1-x}(\text{CN})_6] \cdot n\text{H}_2\text{O}$ for Electroceramic Applications," *J. Alloys and Compounds*, **261**, 182-186 (1997).
28. M. Sakamoto, P. Nunziante, E. Traversa, S. Matsushima, M. Miwa, H. Aono and Y. Sadaoka, "Preparation of Perovskite-Type Oxides by the Thermal Decomposition of Heteronuclear Complexes, $\text{Ln}[\text{Fe}_x\text{Co}_{1-x}(\text{CN})_6] \cdot 4\text{H}_2\text{O}$ (Ln=Pr-Yb)," *J. Ceram. Soc. Jpn.*, **105**, 963-969 (1997).
29. E. Traversa, P. Nunziante, M. Sakamoto, Y. Sadaoka and R. Montanari, "Synthesis and Structural Characterization of Trimetallic Perovskite-Type Oxides, $\text{LaFe}_x\text{Co}_{1-x}\text{O}_3$ by Thermal Decomposition of Cyano-Complexes, $\text{La}[\text{Fe}_x\text{Co}_{1-x}(\text{CN})_6] \cdot n\text{H}_2\text{O}$," *Mater. Res. Bull.*, **33**, 673-681 (1998).
30. F. Hulliger, M. Landolt and H. Vetsch, "Rare-Earth Ferri-

- cyanides and Chromicyanides $\text{LnT}(\text{CN})_6 \cdot n\text{H}_2\text{O}$," *J. Solid State Chem.*, **18**, 283-291 (1976).
31. R. D. Shannon and C. T. Prewitt, "Effective Ionic Radii in Oxides and Fluorides," *Acta Crystallogr. B*, **25**, 925-946 (1969).
 32. R. D. Shannon and C. T. Prewitt, "Revised Values of Effective Ionic Radii," *Acta Crystallogr. B*, **26**, 1046-1048 (1970).
 33. E. Traversa, M. Sakamoto and Y. Sadaoka, "A Chemical Route for the Preparation of Nanosized Rare Earth Perovskite-Type Oxides for Electroceramic Applications," *Particulate Sci. Technol.*, in press (1998).
 34. Y. Sadaoka, H. Aono, E. Traversa and M. Sakamoto, "Thermal Evolution of Nanosized LaFeO_3 Powders from a Heteronuclear Complex, $\text{La}[\text{Fe}(\text{CN})_6] \cdot n\text{H}_2\text{O}$," *J. Alloys and Compounds*, **278**, 135-141 (1998).
 35. S. Venugopalan, M. Dutta, A. K. Ramdas and J. P. Remeika, "Magnetic and vibrational excitations in rare-earth orthoferrites: A Raman scattering study," *Phys. Rev. B*, **31**, 1490-1497 (1985).
 36. S. Venugopalan and M. M. Becher, "Raman scattering study of LuFeO_3 ," *J. Chem. Phys.*, **93**, 3833-3836 (1990).
 37. N. Koshizuka and S. Ushioda, "Inelastic-light-scattering study of magnon softening in ErFeO_3 ," *Phys. Rev. B*, **22**, 5394-5399 (1980).
 38. M. Reedyk, D. A. Crandles, M. Cardona, J. D. Garrett and J. E. Greedan, Raman scattering in the RTiO_3 family of Mott-Hubbard insulators, *Phys. Rev. B*, **55**, 1442-1448 (1997).